J Arid Land (2026) 18(5): 851–867
doi: 10.1016/j.jaridl.2026.05.007; CSTR: 32276.14.JAL.20250492

# Branch architecture of *Tetraena mongolica* Maxim. controls particle size distribution of nebkha sediments

ZHAI Bo[1], DANG Xiaohong[2*], LIU Jing[3], LIU Xiangjie[4], CHEN Xiaona[4], LIU Yajing[4]

[1] School of Geographical Sciences and Planning, Jining Normal University, Ulanqab 012000, China;
[2] College of Desert Science and Engineering, Inner Mongolia Agricultural University, Hohhot 010018, China;
[3] Institute of Water Resources for Pastoral Area of the Ministry of Water Resources of China, Hohhot 010020, China;
[4] Experimental Center for Desert Forestry, Chinese Academy of Forestry, Bayannur 015200, China



**Abstract:** The formation of desert shrub sand piles (nebkhas) is attributed to the obstruction and subsequent deposition of migrating sand by the shrub itself. However, the relationship between sediment particle size distribution and shrub branch architecture remains inadequately understood. In August 2020, field investigations were conducted on *Tetraena mongolica* Maxim. shrubs in the Bayan Engger Desert Nature Reserve, located on the Ordos Plateau in Inner Mongolia Autonomous Region, China. Crown morphological parameters of *T. mongolica* shrubs and associated nebkhas were systematically measured alongside branch architectures. A one-way analysis of variance (ANOVA) was used to identify differences in branch architectures among various levels, while correlation analysis and model fitting were applied to establish the relationship between crown and nebkha morphological parameters. Path analysis was utilized to identify the key branch architectures that influence crown development. Furthermore, sediment redistribution characteristics of nebkhas were quantified, and principal component analysis combined with regression models was utilized to elucidate the contributions of key branch architectures and sensitive particle size fractions to nebkha deposition. Results indicated that the step-by-step branch ratio (SBR) initially increased from the lower branches to the outermost branches before subsequently decreasing. Additionally, branch angle significantly increased ($P$<0.0500), whereas both the branch length and the ratio of branch diameters (RBD) significantly decreased toward the exterior of the shrub ($P$<0.0500). Expansion of crown area significantly enhanced nebkha volume, demonstrating a strong linear relationship ($P$<0.0010). As the primary contact surface for trapping wind-blown sand, the silhouette area of the shrub initially increased and then decreased from bottom to top. Notably, the silhouette area of the 10–30 cm height layer played a crucial role in promoting nebkha volume expansion ($P$<0.0100). Path analysis further revealed that the key branch architectures promoting crown area expansion were the step-by-step branch ratio between the third-level and fourth-level branches ($SBR_{3:4}$), followed by the fourth-level branch length ($BL_{L4}$), the third-level branch angle ($BA_{L3}$), and the ratio of branch diameters between the fourth-level and third-level branches ($RBD_{4:3}$). Under the continuous interception of sediments by branches and leaves, the proportion of surface sediment with a particle size of 100.00–250.00 μm reached 51.07%, indicating a significant increase in fine-sized particles. Further analysis confirmed that $SBR_{3:4}$, $BL_{L4}$, $BA_{L3}$, and sediments within the 50.00–100.00 μm particle size range were the primary contributors to nebkha deposition. These results demonstrate that the branch characteristics of *T. mongolica* shrubs near the ground surface promote fine sediment accumulation and nebkha development by regulating crown expansion. The findings reveal the unique adaptation mechanisms of rare and endangered plants in nebkha microhabitats and provide a scientific basis for ecological windbreak and sand-fixation projects in the desert transition zones of arid and semi-arid regions.

*Corresponding author: DANG Xiaohong (E-mail: dangxiaohong1986@126.com)
Received 2025-10-10; revised 2026-03-27; accepted 2026-03-30

**Keywords:** *Tetraena mongolica* Maxim.; nebkhas; branch architecture; particle size distribution; nebkha formation; Ordos Plateau

**Citation:** ZHAI Bo, DANG Xiaohong, LIU Jing, LIU Xiangjie, CHEN Xiaona, LIU Yajing. 2026. Branch architecture of *Tetraena mongolica* Maxim. controls particle size distribution of nebkha sediments. Journal of Arid Land, 18(5): 851–867. https://doi.org/10.1016/j.jaridl.2026.05.007; https://cstr.cn/32276.14.JAL.20250492

## 1 Introduction

The plant modular theory is a fundamental concept in morphology and ecology, proposing that the growth patterns of most individuals at any life stage can be expressed through architectural features (White, 1979; Savinov, 2020). These configurations—representing a plant's external structure—comprise various components originating from growth and adaptation and reflect the interaction between the plant and its environment (Bazzaz, 1979; Dos Santos et al., 2022).

Branch architecture is a central focus of plant crown analysis (Araus et al., 2022). It influences the complexity of shrub canopies by determining the arrangement of branches and leaves (Koller et al., 2025). Exploring the relationship between branch patterns and morphology can enhance our understanding of the ecological strategies adopted by plant populations. According to Chambers (2020), this adaptability mediates how plants impact their geomorphic and climatic environment and vice versa, providing a theoretical backdrop to comprehend species evolution. Three morphological features primarily determine branch patterns: bifurcation ratio, branch angle, and branch length (Honda, 1971; Leopold, 1971; Steingraeber et al., 1979).

While previous studies have extensively examined the relationship between plant crown morphology and biomass in humid and sub-humid regions, the effects of branch architecture on plant growth in arid and semi-arid environments remain poorly understood (Fisher and Honda, 1979; Enquist et al., 1998; Valladares et al., 2007; Niklas and Cobb, 2010; Hildebrand et al., 2021; Yan et al., 2025). Through long-term adaptation, desert shrubs have developed unique growth strategies, including resistance to wind erosion, sand abrasion, burial, and drought (Wu et al., 2023). Compared to vegetation in other regions, desert shrubs play a unique role in windbreaking and sand fixation. Their efficiency primarily depends on their morphology in relation to wind direction; changes in branch architecture can alter the crown size and, consequently, the shape of the windward side (Pang et al., 2022). These plants capture aeolian sand grains through their aboveground branches and leaves, depositing them to form "nebkhas" (Costas et al., 2024). Existing studies indicate that vegetation characteristics control deposition, and that shrub branch architecture determines both sediment accumulation and the morphology of the underlying sand dune (e.g., Zhang et al., 2020). Therefore, a thorough understanding of these influences is crucial for successful sand control and vegetation restoration.

*Tetraena mongolica* Maxim., a relict shrub from the ancient Mediterranean flora, represents the sole species within the monotypic Zygophyllaceae subfamily Tetraenoideae. It is found exclusively in China, thriving in dry, sandy habitats characterized by high temperatures and windy conditions (Xu et al., 2023). Given that these ecosystems are particularly vulnerable to natural geographical shifts (Xu et al., 2020), clarifying the relationship between *T. mongolica* and its environment can provide a vital theoretical basis for the ecological restoration.

Desertification has been a persistent environmental issue on the Ordos Plateau in Inner Mongolia Autonomous Region, China (Hu et al., 2021). Desert shrubs play a pivotal role in shaping the ecological dynamics of this region, where they serve as foundational species in maintaining biodiversity, ecosystem stability, and soil fertility. They are also key elements in the formation of nebkhas—distinctive aeolian landforms characterized by sand accumulation around vegetation (Li and Ravi, 2018; Li et al., 2019). The interaction between shrubs and aeolian sediment transport drives this process. Because aboveground branch architecture directly influences nebkha formation (Hesp, 1981; Wolfe and Nickling, 1993), exploring this relationship is essential for understanding shrub rejuvenation and preventing desertification (Lu et al., 2023; Zhu et al., 2024).

Current studies on *T. mongolica* primarily concentrate on its landscape patterns and anatomical changes in its leaves, xylem, and phloem. To understand the relationship between branch architecture and sediment characteristics during nebkha formation, this study quantifies the association between plant size and nebkha dimensions and analyzes the contributions of shrub configuration to sedimentary development. Based on these objectives, this study proposes the following three hypotheses: (1) significant differences exist in the branch morphology among different branch levels; (2) the overall branch architecture of the shrub shows a positive correlation with nebkha size; and (3) some primary branch architectures promote nebkha accumulation by influencing the particle size distribution of deposited sediments. The findings can provide a theoretical foundation for the artificial regulation of shrub branch architecture to achieve optimal wind-resistant and sand-fixing effects.

## 2 Materials and methods

### 2.1 Study area

The Bayan Engger Desert Nature Reserve (107°10′51.24″E, 40°15′49.71″N), located in Hanggin Banner on the Ordos Plateau, Inner Mongolia Autonomous Region, China, was selected as the study area. Situated at the transition zone between grasslands and shrublands, this region faces severe challenges from desertification. The climate is typically semi-arid, characterized by pronounced seasonal and diurnal temperature variations. The annual average temperature is 5.6°C, and the average annual precipitation is 144.6 mm. The area is primarily influenced by northwesterly winds, which reach an average speed of 4.1 m/s and result in approximately 27.8 d of strong winds annually. The Bayan Engger Desert Nature Reserve extends approximately 28 km north–south and 20 km east–west, comprising three soil types: grey desert, aeolian sand, and coarse skeletal soils. The nature reserve hosts 58 varieties of endemic, relict, and endangered species, representing 17.80% of its total flora. Among these, rare and endangered taxa such as *T. mongolica*, *Helianthemum songaricum* Schrenk ex Fisch. & C. A. Mey., *Potaninia mongolica* Maxim., and *Ammopiptanthus mongolicus* (Maxim. ex Kom.) S. H. Cheng are particularly prominent.

### 2.2 Morphometric measurements of shrubs and nebkhas

Field investigations were conducted in August 2020 within the experimental zone of the study area. To examine intraspecific processes under isolated conditions, we established three intensively monitored plots (each measuring 20 m×20 m) within nearly monospecific stands of *T. mongolica*. This natural control design effectively eliminated the confounding effects of interspecific competition, thereby enabling the precise quantification of autonomous growth and nebkha dynamics of *T. mongolica*. A total of 20 shrubs were randomly selected from each plot as analytical samples, resulting in a total of 60 individuals across all plots. For every selected *T. mongolica* shrub and its respective nebkha (Fig. 1), we used a steel tape to measure the following dimensions: shrub crown length (cm), width (cm), and height (cm), as well as nebkha length (cm), width (cm), and height (cm). The length was defined as the longest axis, while the perpendicular axis was designated as the width. To calculate the crown area ($cm^2$), we applied the formula for the area of an ellipse: crown area=[π(crown length×crown width)]/4. The nebkha bottom area ($cm^2$) was also calculated using the formula for the area of an ellipse: nebkha bottom area=[π(nebkha length×nebkha width)]/4. Finally, the nebkha volume ($cm^3$) was calculated using the formula for the volume of a hemiellipsoid: nebkha volume=[π(nebkha length×nebkha width× nebkha height)]/6 (Liu et al., 2009).

### 2.3 Determination of shrub silhouette area

We photographed the experimental shrubs with a Nikon COOLPIX S8100 camera (Nikon Corporation, Tokyo, Japan) from the upwind side along the prevailing wind direction, starting at ground level. The distance between the camera and the windward edge of the shrub was

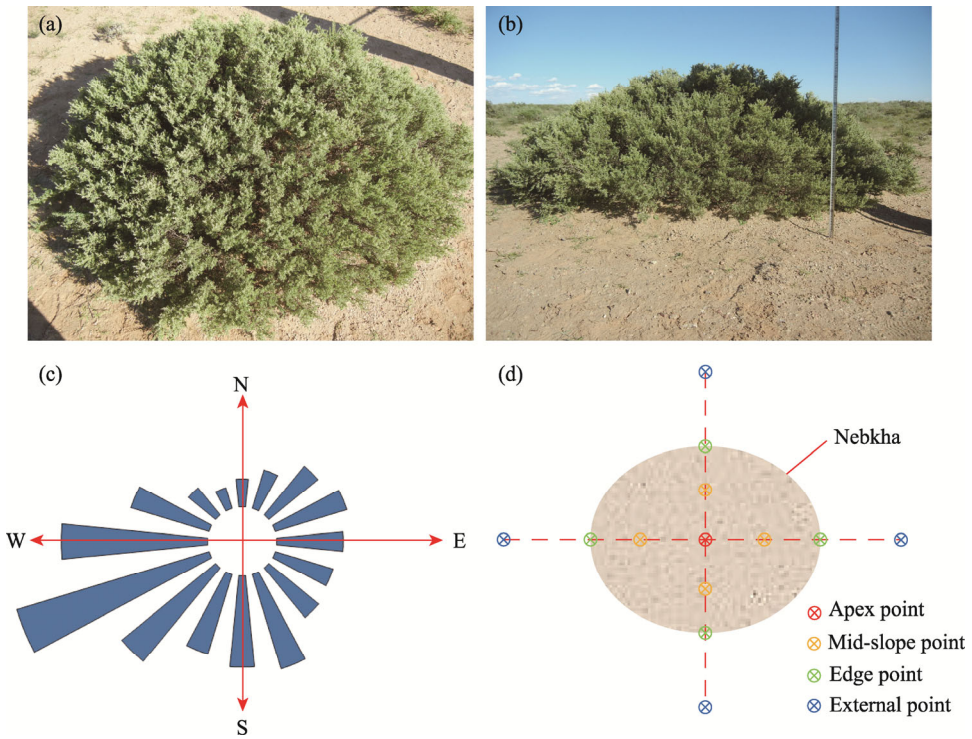


**Fig. 1** Photographs showing the *Tetraena mongolica* Maxim. (a) and its nebkha (b), the annual wind rose diagram of the study area (c), and a schematic diagram indicating sampling points for collecting sediments from individual nebkhas (d). N, north; S, south; W, west; E, east.

maintained at 3 m. A straight ruler was placed on the shrub's windward side to provide a scale while filming the entire windward side of the shrub. Silhouette areas were measured separately at the height intervals of 0–10, 10–30, and 30–50 cm. When a shrub's height exceeded 50 cm, the silhouette area above the 50 cm mark was also measured. The silhouette photos were imported into the AutoCAD 2007 software (Autodesk, Inc., San Rafael, USA), where the contours and gaps of each height layer on the shrub's windward side were outlined. Using the area calculation function in the software, we identified the gap and overall contour area for each height layer, and calculated their ratio to obtain the porosity of the windward surface. Finally, the silhouette area ($cm^2$) of each height layer was calculated using the following formula: silhouette area of height layer=trapezoid area of height layer×(1–porosity) (Chang et al., 2017).

### 2.4 Determination of shrub branch architecture

The aboveground branch architecture of the 60 selected shrubs were determined using the centripetal method (Borchert and Slade, 1981). Under this system, the outermost branch was classified as the first-level branch. When two first-level branches converged, the resulting segment was defined as a second-level branch; this pattern continued sequentially, with near-surface branches classified as the highest-level branches. The total number of branches at each level was recorded and a steel tape was used to determine the branch lengths. Pro'sKit PD-301 digital vernier calipers (0.01 mm resolution; Prokit's Industries Co., Ltd., Taipei, China) were used to measure the branch diameters at all levels. The branch angles were measured at all levels using a protractor. The overall branch ratio (OBR), step-by-step branch ratio (SBR), and the ratio of branch diameters (RBD) were calculated using the following formulas:

$$\mathrm{OBR}=\left(N_T-N_S\right)/\left(N_T-N_1\right), \quad (1)$$

$$\mathrm{SBR}_{i,i+1}=N_i/N_{i+1}, \quad (2)$$

$$\mathrm{RBD}=D_{i+1}/D_i, \quad (3)$$

where $N_T$ is the total number of branches at all levels; $N_S$ is the number of branches with the highest level; $N_1$ is the number of the first-level branches; $SBR_{i,\,i+1}$ is the step-by-step branch ratio between the $i^{th}$-level and $(i+1)^{th}$-level branches; $N_i$ and $N_{i+1}$ are the total numbers of branches at the $i^{th}$ level and $(i+1)^{th}$ level, respectively; and $D_i$ and $D_{i+1}$ denote the diameters of the $i^{th}$-level and $(i+1)^{th}$-level branches (cm), respectively.

### 2.5 Sediment collection from the nebkhas

Within each surveyed plot, we selected eight nebkhas based on the investigated shrub crown area, totaling 24 nebkhas across the three plots. This was done to systematically collect sediment samples from each of these nebkhas. For each nebkha, two perpendicular transects were established along the long and short axes. Along each transect, four sampling position types were designated: (1) the apex of the nebkha (one sampling point); (2) the mid-slope between the apex and the edge (two sampling points); (3) the edge of the nebkha (two sampling points); and (4) external points located 50 cm beyond the nebkha edge (two sampling points) (Fig. 1). Sediment samples were collected from each sampling point at a depth interval of 0–10 cm. To facilitate comparative analysis, we categorized the collected samples into three distinct groups: samples from the apex and mid-slope sampling points were combined to represent the interior of the nebkha; samples from the edge sampling points were pooled to represent the base of the nebkha; and samples collected 50 cm from the edge were integrated to represent the external environment. A total of 24 sediment samples (eight nebkhas×three sediment groups) were collected from each plot, resulting in 72 sediment samples for the three plots combined.

### 2.6 Sediment analysis

Sediment samples were treated with $H_2O_2$ (30.00% mass concentration) to eliminate organic matter. To disperse the aggregates, we added sodium hexametaphosphate (NaHMP) and subjected the samples to sonication for 30 s. Sample analysis was performed using laser diffraction technology with a laser particle size analyzer (Analysette 22 Micro Tec Plus; Fritsch GmbH, Idar-Oberstein, Germany). This analyzer enables the measurement of particle size distribution values ranging from 0.01 to 2000.00 μm, providing a continuous volume fraction of particle sizes during the analysis.

### 2.7 Statistical analysis

Before performing statistical analysis, we assessed all variables for normality using the Kolmogorov–Smirnov test. This study established a regression equation between the crown area of *T. mongolica* and nebkha characteristics. We used SPSS 17.0 software (SPSS Inc., Chicago, USA) to conduct a one-way analysis of variance (ANOVA) on the silhouette area and branch architecture of shrubs with different sizes. Correlation analysis was conducted between shrub characteristics (silhouette area and branch architecture) and nebkha morphological indicators. We performed stepwise regression analysis and path analysis on the branch architecture and crown area of *T. mongolica* shrubs. The decision coefficient served as the decision index in the path analysis (Awogbemi et al., 2022). By calculating the decision coefficient, we comprehensively ranked the influence of the corresponding independent variables and determined the main decision variables. The formula is as follows:

$$DC=2P_j\times r_{jy}-P_j^2, \tag{4}$$

where DC is the decision coefficient; $P_j$ is the direct path coefficient of the independent variable $j$; and $r_{jy}$ is the correlation coefficient between the independent variable $j$ and the dependent variable $y$. When decision coefficient>0, the independent variable has an enhancing effect on the dependent variable; when decision coefficient<0, the independent variable has an inhibitory effect on the dependent variable.

The residual factor in the stepwise regression analysis can describe the comprehensiveness of the selected model consideration. The formula is as follows:

$$e=\sqrt{\left(1-R^2\right)}, \tag{5}$$

where $e$ is the residual factor; and $R^2$ is the degree of fit of the stepwise regression equation. When the value of residual factor is small, the independent variables selected in the stepwise regression equation are considered more comprehensively.

Based on the sediment particle size classification system established by the United States Department of Agriculture (USDA), we identified seven fractions of sediment particle sizes: <2.00, 2.00–50.00, 50.00–100.00, 100.00–250.00, 250.00–500.00, 500.00–1000.00, and 1000.00–2000.00 μm. The proportion of each particle size was calculated and reported. Principal component analysis (PCA) was performed using SPSS 17.0 software on the key branch architectures of the shrubs from which the sediment was collected, as well as on the sediment content of each particle size fraction in the surface layer of nebkhas.



## 3 Results

### 3.1 Branch characteristics of *T. mongolica* shrubs

The branch pattern of the shrub's shoots determines the expansion of both the shrub's middle and upper layers. Hence, we first analyzed the branch characteristics across all levels. The OBR and SBR of the selected plant samples were measured and counted, revealing an overall branch ratio of 4.90. The SBR from the branches near the shrub's lower part to the outermost branches initially increased and then decreased. Among them, the step-by-step branch ratio between the second-level and third-level branches ($SBR_{2:3}$) was significantly higher than those in the other branches ($P$<0.0500; Table 1). Measurements of branch length, branch angle, and RBD were conducted on shrub samples. As the hierarchy of branches increased from outer to basal branches, both branch length and RBD exhibited a gradual increase, whereas branch angle demonstrated a progressive decrease (Fig. 2).

**Table 1** Single-factor variance analysis of the overall and stepwise branch ratios of *Tetraena mongolica* Maxim.

| | OBR | $SBR_{1:2}$ | $SBR_{2:3}$ | $SBR_{3:4}$ |
|---|---|---|---|---|
| Branch ratio | 4.90±0.68 | 4.79±0.81$^b$ | 5.79±0.95$^a$ | 4.51±1.02$^b$ |

Note: Mean±SD ($n$=60). OBR, overall branch ratio; $SBR_{1:2}$, step-by-step branch ratio between the first-level and second-level branches; $SBR_{2:3}$, step-by-step branch ratio between the second-level and third-level branches; $SBR_{3:4}$, step-by-step branch ratio between the third-level and fourth-level branches. Different lowercase letters indicate significant differences in the branch ratios between different branch levels ($P$<0.0500).

### 3.2 Relationship between overall shrub morphology parameters and nebkha size

The linear regression equation connecting the crown area of *T. mongolica* shrubs with nebkha bottom area can be expressed as $y_1$=0.83$x$–0.40 (where $y_1$ is the nebkha bottom area and $x$ is the shrub crown area), with an $R^2$ value of 0.94 and a $P$-value of less than 0.0010 (Fig. 3a). Analysis through linear regression indicated a strong positive correlation between shrub crown area and nebkha bottom area. The linear regression equation between shrub crown area and nebkha volume was: $y_2$=0.20$x$–0.18 (where $y_2$ is the nebkha volume) ($R^2$=0.81, $P$<0.0010; Fig. 3a). The residuals of the linear equations were all normally distributed. These results showed that the crown structure in desert shrubs significantly influences the formation and morphology of nebkhas, with the crown area being the primary morphological index for shrubs. As shown in Figure 3b, the crown length, width, and height of shrubs were significantly positively correlated with the corresponding morphological parameters of nebkha ($P$<0.0010). Among these parameters, crown length exhibited the highest correlation coefficient with both nebkha length and width at 0.97, whereas crown height demonstrated the lowest correlation coefficient with nebkha height at 0.63.

The shrub's windward side is the key contact surface affecting nebkha development; therefore, changes in the silhouette area of the windward side are crucial. We divided the profile of *T. mongolica* into three height layers and calculated the silhouette area of each height layer for all

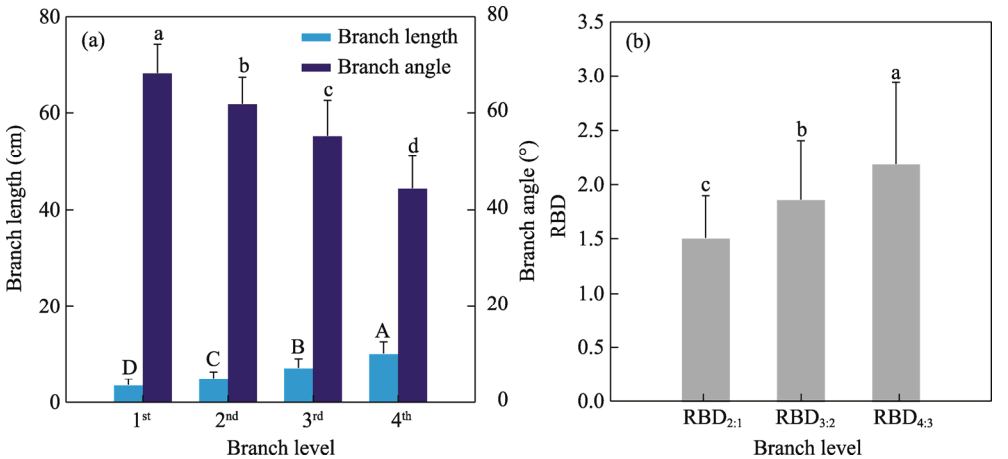


**Fig. 2** Branch length and angle ($n$=60; a) and the ratio of branch diameters (RBD) across the four branch levels ($n$=60; b) of *T. mongolica* shrubs. On the $x$-axis of the left panel, the 1st, 2nd, 3rd, and 4th refer to the first-level to fourth-level branches, respectively. $RBD_{2:1}$, ratio of branch diameters between the second-level and first-level branches; $RBD_{3:2}$, ratio of branch diameters between the third-level and second-level branches; $RBD_{4:3}$, ratio of branch diameters between the fourth-level and third-level branches. Error bars mean standard deviations. Different uppercase letters indicate significant differences in branch length between different branch levels ($P$<0.0500); different lowercase letters indicate significant differences in branch angle or RBD between different branch levels ($P$<0.0500).

shrubs. Using a one-way ANOVA, we found significant differences among the silhouette areas of the three height layers ($P$<0.0500; Table 2). Among these, the silhouette area of the 10–30 cm height layer was significantly higher than that of the other height layers ($P$<0.0500). The correlation heat map revealed that the silhouette area of the shrubs' windward side was significantly and positively correlated with nebkha bottom area and volume ($P$<0.0100; Fig. 4). Specifically, the silhouette area of the 10–30 cm height layer demonstrated the highest correlation coefficient with nebkha bottom area (correlation coefficient=0.82), exceeding those of all other height layers. With a correlation coefficient of 0.95, the silhouette area of the 30–50 cm height layer had the most significant influence on the total silhouette area compared to the other height layers. The correlation coefficient between the silhouette area of the 10–30 cm height layer and nebkha volume was 0.81, which was higher than that of the 0–10 and 30–50 cm height layers. Therefore, the silhouette area of the 10–30 cm height layer was the key contact surface for regulating shrub expansion and promoting nebkha development.

### 3.3 Path analysis of shrub branch architecture and crown area

Stepwise regression analysis was used to screen the branch architecture indicators that affected the crown area of *T. mongolica* shrubs. As the independent variables were gradually introduced into the regression equation, the $R^2$ of the equation increased. Calculations revealed that the residual factor was 0.25. This value was small, confirming that the influence of the selected independent variables on the crown area was more pronounced. Four independent variables of branch architecture were screened out in the model summary table: the fourth-level branch length ($BL_{L4}$), step-by-step branch ratio between the third-level and fourth-level branches ($SBR_{3:4}$), the third-level branch angle ($BA_{L3}$), and the ratio of branch diameters between the fourth-level and third-level branches ($RBD_{4:3}$). The crown area was defined as the dependent variable, and the other parameters was regarded as the independent variables. The optimal multiple regression equation was established as follows: $y$=1451.41$x_1$+3507.17$x_2$+411.20$x_3$–1650.54$x_4$–25411.52 (where $y$ is the shrub crown area, $x_1$ is the $BL_{L4}$, $x_2$ is the $SBR_{3:4}$, $x_3$ is the $BA_{L3}$, and $x_4$ is the $RBD_{4:3}$; $R^2$=0.94, $P$=0.0400). The one-way ANOVA results based on crown area data showed a significant effect ($F$=90.38, $P$≤0.0010), and the residuals followed a normal distribution. Consequently, the stepwise regression equation can be deemed statistically significant.

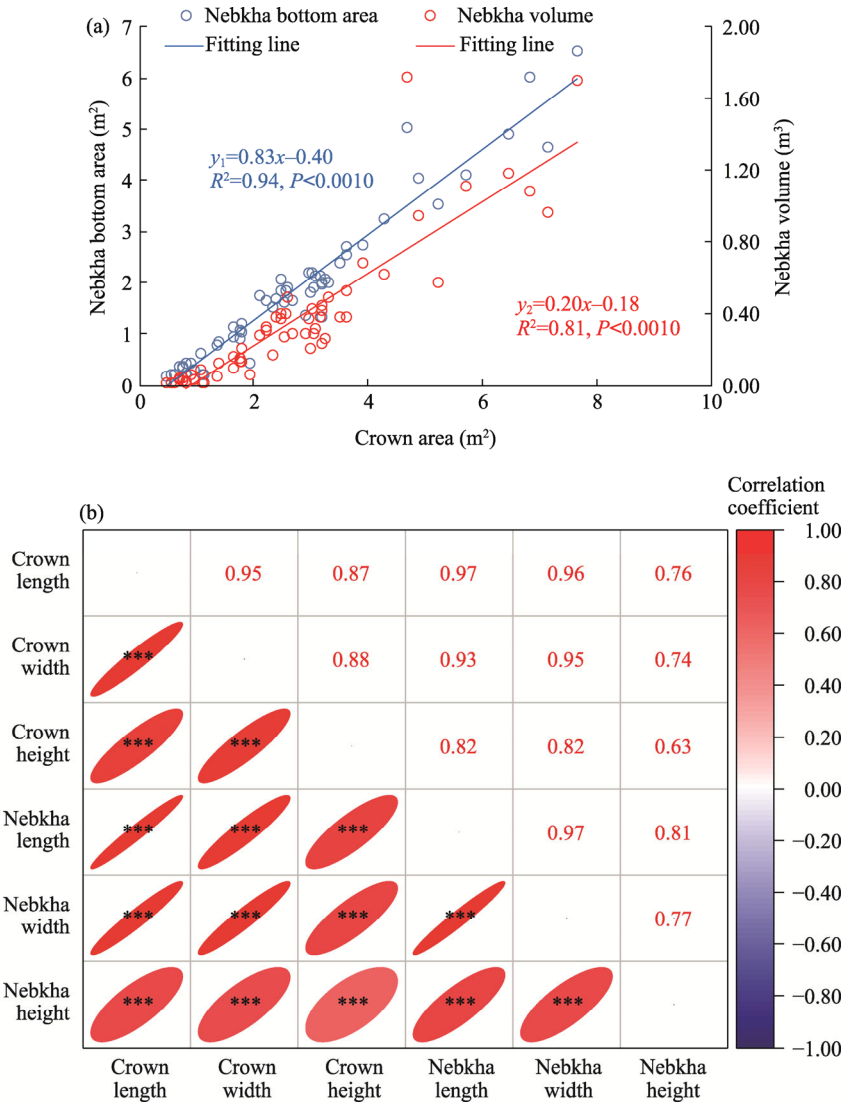


**Fig. 3** Fitting relationship of the crown area of *T. mongolica* shrubs with nebkha bottom area and volume (a), and correlation analysis between shrub morphological parameters and nebkha morphological indices. ***, $P$<0.0010 level. The flatter the red ellipse, the stronger the correlation.

**Table 2** Silhouette area of each height layer of *T. mongolica* shrubs and the total shrub silhouette area

| | 0–10 cm height layer | 10–30 cm height layer | 30–50 cm height layer | Total |
|---|---|---|---|---|
| Silhouette area (m²) | 1.30±0.43$^c$ | 3.10±0.89$^a$ | 2.38±1.08$^b$ | 7.48±3.84 |

Note: Mean±SD ($n$=60). Different lowercase letters indicate significant differences in the silhouette area among different height layers of *T. mongolica* shrubs ($P$<0.0500).

We conducted a path analysis between the key branch architecture parameters selected in the previous step and crown area (Fig. 5). Our findings indicated that the direct path coefficients were as follows: $BL_{L4}$=0.33, $SBR_{3:4}$=0.35, $BA_{L3}$=0.29, and $RBD_{4:3}$= –0.12. Variables $BL_{L4}$, $SBR_{3:4}$, and $BA_{L3}$ exerted direct positive effects on canopy area, whereas $RBD_{4:3}$ exerted a direct negative effect on canopy area. The decision coefficients revealed that the order of the main branch architectures affecting the crown area was as follows: $SBR_{3:4}$>$BL_{L4}$>$BA_{L3}$>$RBD_{4:3}$, indicating that the branch ratio near the ground surface is the most crucial branch architecture factor determining the shrub crown area.

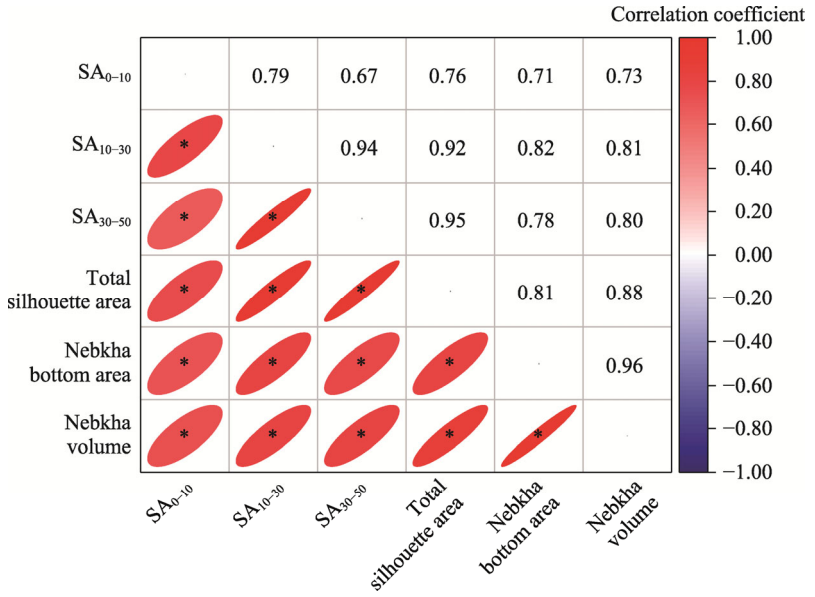


**Fig. 4** Correlation analysis of shrub silhouette area with nebkha bottom area and volume. $SA_{0–10}$, $SA_{10–30}$, and $SA_{30–50}$ represent the silhouette areas of the 0–10, 10–30, and 30–50 cm height layers of *T. mongolica* shrubs, respectively. *, $P<0.0100$ level. The flatter the red ellipse, the stronger the correlation.

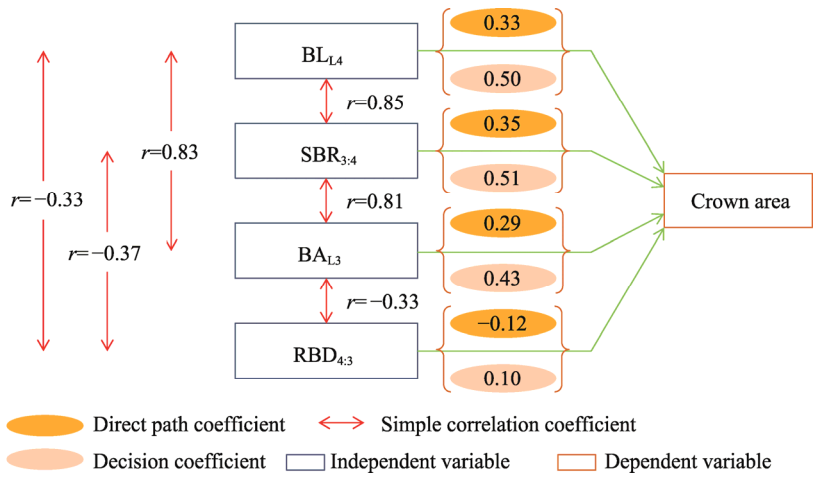


**Fig. 5** Path analysis showing the relationship between branch architecture and crown area of *T. mongolica* shrubs. $BL_{L4}$, fourth-level branch length; $SBR_{3:4}$, step-by-step branch ratio between the third-level and fourth-level branches; $BA_{L3}$, third-level branch angle; $RBD_{4:3}$, ratio of branch diameters between the fourth-level and third-level branches; *r*, correlation coefficient.

### 3.4 Contribution of primary shrub branch architectures and sediment redistribution to nebkha formation

The internal and external sediment textures of the nebkha indicated that the distribution patterns of sediment particle sizes at various positions were consistent (Fig. 6). In the surface sediments located in the interior and exterior of the nebkha, the content of fine sand, particularly in the particle size range of 100.00–250.00 μm, was the highest. This particle size category demonstrated the greatest content within the surface sediments of the nebkha, with a proportion of 51.07% for particles sized 100.00–250.00 μm, followed by sediments from the base, whereas the external area exhibited the lowest content. Upon moving further away from the nebkha, the content of fine sand progressively decreased. Additionally, in the surface layer of the nebkha,

sediment with a particle size ranging from 50.00 to 100.00 μm was found to be more abundant than that in both the base and exterior of the nebkha. Furthermore, sediment particles measuring 2.00–50.00 μm had a lower content within the nebkha than in the external area.

The branch architecture of shrubs affects sediment distribution, thereby influencing the accumulation of nebkhas, a phenomenon that can be well-explained by PCA. We conducted PCA on the primary shrub branch architectures related to nebkha development and the particle size composition of nebkha surface sediments. Three principal components were extracted, accounting for a cumulative contribution rate of 80.20% (Table 3). The principal component loadings for each indicator, which represent the correlation coefficients between each indicator and the relevant principal components, are shown in Table 3.

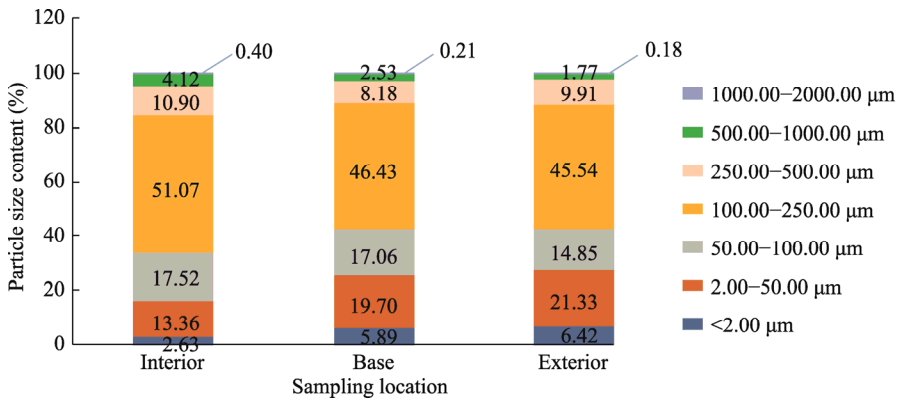


**Fig. 6** Comparison of sediment structures among the interior, base, and exterior of the nebkha

**Table 3** Principal component analysis (PCA) of nebkha formation based on the branch architectures of *T. mongolica* shrubs and intercepted sediment fractions

| Indicator | Principal component loading | | |
|---|---|---|---|
| | PC1 | PC2 | PC3 |
| $BL_{L4}$ | 0.87 | 0.30 | 0.20 |
| $SBR_{3:4}$ | 0.95 | 0.11 | 0.10 |
| $BA_{L3}$ | 0.91 | 0.19 | 0.12 |
| $RBD_{4:3}$ | –0.37 | 0.11 | –0.16 |
| <2.00 μm | –0.46 | –0.72 | 0.35 |
| 2.00–50.00 μm | 0.02 | –0.82 | 0.51 |
| 50.00–100.00 μm | 0.93 | 0.07 | 0.14 |
| 100.00–250.00 μm | 0.52 | –0.10 | –0.58 |
| 250.00–500.00 μm | –0.41 | –0.14 | –0.71 |
| 500.00–1000.00 μm | –0.67 | 0.66 | 0.33 |
| 1000.00–2000.00 μm | –0.64 | 0.69 | 0.31 |
| Contribution rate (%) | 45.44 | 20.70 | 14.06 |
| Accumulated contribution rate (%) | 45.44 | 66.14 | 80.20 |

Note: $BL_{L4}$, fourth-level branch length; $BA_{L3}$, third-level branch angle; $RBD_{4:3}$, ratio of branch diameters between the fourth-level and third-level branches; PC1, first principal component; PC2, second principal component; PC3, third principal component.

Results indicated that during the process of nebkha accumulation, the first principal component (PC1) accounted for 45.44% of the variance, and the second principal component (PC2) occupied 20.70%. In the PC1 loading, the values for $SBR_{3:4}$, $BL_{L4}$, $BA_{L3}$, and 50.00–100.00 μm particle size fraction were notably high. Therefore, the main branch architectures of $SBR_{3:4}$, $BL_{L4}$, and $BA_{L3}$ from the PC1 were selected as the independent variables, and the sediment content within

the particle size range of 50.00–100.00 μm and nebkha volume were designated as the dependent variables, for establishing the regression equations (Table 4). Results implied that the branch architectures of $SBR_{3:4}$, $BL_{L4}$, and $BA_{L3}$ effectively increased the sediment content in the 50.00–100.00 μm range, thereby facilitating the development and stabilization of nebkhas.

**Table 4** Fitting equations relating the main branch architectures of *T. mongolica* shrubs with sediment particle size and nebkha volume

| No. | Equation | $R^2$ | $P$ | $F$ |
|---|---|---|---|---|
| 1 | $y_1=3.26x_1+2.52$ | 0.87 | 0.0001 | 143.47 |
| 2 | $y_1=1.22x_2+4.99$ | 0.68 | 0.0001 | 46.22 |
| 3 | $y_1=0.48x_3-8.93$ | 0.72 | 0.0001 | 55.81 |
| 4 | $y_2=268066x_1-850373$ | 0.64 | 0.0001 | 39.57 |
| 5 | $y_2=106430x_2-712955$ | 0.57 | 0.0001 | 29.02 |
| 6 | $y_2=106430x_3-1619457$ | 0.45 | 0.0001 | 18.03 |

Note: $y_1$, content of sediments with particle size of 50.00–100.00 μm; $y_2$, nebkha volume; $x_1$, $SBR_{3:4}$ (step-by-step branch ratio between the third-level and fourth-level branches); $x_2$, $BL_{L4}$ (fourth-level branch length); $x_3$, $BA_{L3}$ (third-level branch angle).

## 4 Discussion

### 4.1 Influence of branch architecture of *T. mongolica* on its canopy development

Architectural plasticity in woody plants reflects a dynamic equilibrium between resource capture and competitive avoidance, wherein branch length, ratio, and angle exhibit concerted adjustments to microenvironmental heterogeneity (Clark and Ma, 2023; Zhao et al., 2025). For *T. mongolica* shrubs, this tripartite coordination yields a distinctive spatial gradient: branch length diminishes acropetally, with maximal extension concentrated in the near-surface stratum (approximately 20 cm above ground), whereas the ratio of branch diameter intensifies basally. This pattern arises from the ontogenetic differentiation between long shoots—which feature extended internodes that facilitate lateral crown expansion—and short shoots with compressed internodes that optimize leaf display while mitigating self-shading and mechanical abrasion from stem-on-stem contact (Yagi, 2006). The functional implications of this architecture are evident in the adjustments of branch angles that reallocate growth priorities. An increased inclination of peripheral branches diminishes vertical apical dominance while enhancing lateral crown spread (Osada, 2006). Concurrently, increases in basal diameter ratios enhance the mechanical stability necessary to support this expanded architecture (He et al., 2005).

Branch architecture fundamentally constrains crown morphology in woody plants, with branch ratio denoting the proportion between successive branch levels serving as a crucial index of structural complexity (Yang et al., 2022). Earlier studies proposed that the bifurcation ratio is stable and species-specific (e.g., Whitney, 1976), but recent evidence indicates substantial ontogenetic plasticity within these branch ratios, as they dynamically change throughout growth period (Qu et al., 2022). According to conventional theory, crown morphology is mainly determined by branch patterns in the periphery of temperate deciduous species. The outer leaves determine the outline of the tree (Steingraeber and Waller, 1986). However, this paradigm needs revision for *T. mongolica* because its branches are densely covered with oblanceolate leaves. Hence, the architectural determinants of shrubs should be assessed based on the branch ratios near the main stem (Barthélémy and Caraglio, 2007). This research demonstrated that branch ratios from the ground surface of *T. mongolica* shrubs hold excessive control over shrub morphology. The characteristic acropetal tapering from base to apex generates a windward profile that systematically modulates incident wind speed, entraining airflow into turbulent wakes that accelerate along both flanks. Crucially, the lower stratum produces the most extensive disturbance zone due to maximal branch density and three-dimensional complexity. The near-surface branches

serve dual functions, acting as a structural scaffold for crown expansion and as an aerodynamic baffle that induces flow separation and sediment entrapment. Consequently, the densely branched middle layer emerges as the primary locus of sediment deposition, with branch complexity directly mediating trapping efficacy (Qu et al., 2022). This functional linkage suggests that the branch architecture of *T. mongolica* may represent an adaptive compromise between light interception and aeolian sediment capture, a hypothesis warranting comparative investigation across species with divergent branch strategies.

### 4.2 Relationship between the canopy structure of *T. mongolica* and the corresponding nebkha size

*T. mongolica*, an important foundational species in the desert transition zones (Liu et al., 2023), plays a crucial role in windbreak maintenance and sand immobilization. Understanding the influence of its canopy morphology on nebkha development and sediment distribution is essential for elucidating the mechanisms of aeolian sediment trapping in arid and semi-arid environments. Previous studies have demonstrated that variations in plant growth form and canopy porosity significantly affect nebkha morphology and sediment accumulation patterns (El-Sheikh et al., 2010; Li et al., 2021; Ciancio et al., 2022; Goudie, 2022). As a small shrub species, *T. mongolica* thrives in desert transition zones and leads to the development of stable shrub-dominated landforms. Its crown usually assumes a hemispherical structure that encompasses a major part of the nebkha surface. This morphological characteristic confers it greater sand-trapping efficiency than other shrubs, as evident from its higher sediment retention (Cheng et al., 2018).

A positive linear relationship between the crown area of *T. mongolica* and nebkha volume was identified (Fig. 3a). The findings were confirmed via wind tunnel erosion experiments conducted later (Fig. S1). This shrub species significantly disturbed the saltation-laden airflow, with the mean wind speed at 0–20 cm height declining significantly just downstream of the crown, coupled with the sand-transport rate being reduced by more than 70.00% relative to the upstream surface. As the transport capacity diminished, swift deposition of intercepted particles ensued, resulting in nebkha formation with the classic wind-shadow morphological development. The shrub patches can potentially initiate and stabilize dune-like accumulations through their interactions with the simulated near-surface flow, by enhancing sediment retention (Zhai, 2022). Mature plants with a solid hemispherical crown on the windy side, such as *Nitraria tangutorum* Bobrov, produce the larger nebkha (Zhang et al., 2020). The relatively low height to width ratio of the structure causes protrusion of flow towards the upper surface and generates low velocity wake force, leading to deposition (Qu et al., 2011; Kidron and Zohar, 2016; Cheng et al., 2018; Li and Ravi, 2018). The silhouette area of the 10–30 cm height layer was most strongly related to nebkha volume, supporting the view that thickets with a windward profile centroid less than 30 cm above the ground surface most effectively contribute to stable nebkha formation (Chang et al., 2017). These observations revealed that nebkha accumulation around *T. mongolica* is not merely a passive consequence of canopy presence, but rather an emergent property of strategically optimized branch geometry. By concentrating architectural complexity in the middle layer, the shrub maximizes its basal silhouette area, thereby creating persistent vortices that preferentially deposit sediments. This functional stratification underscores that sediment capture efficiency is directly modulated by the targeted deployment of branches in the near-surface layer, where wind velocity reduction and particle deposition are most pronounced.

### 4.3 Contribution of key branch architectures and sediment particle size redistribution to nebkha accumulation

Through the process of aeolian sorting, particle size distributions on the surface dynamically redistribute, whereby vegetation serves as a geomorphic filter that assists in particle transport diffusion by trapping particles with uneven efficiency. Nebkha sediments originate from short-range saltation and suspension. The grain size spectra of these sediments reflect the wind energy regimes at the site. Enrichment of coarser fractions indicates a strong transportation capacity, whereas fine-dominated particles indicate a weak transportation capacity; such

sediments are a proxy for vegetation effectiveness in site stabilization (Tengberg, 1995; Guan et al., 2013). In desert environments, particles with diameters less than 400.00 μm constitute the most erodible fraction of the sediments. Such a highly sensitive component is thus the primary driving factor of local sedimentological heterogeneity. Saltation occurs for particles in the 70.00–500.00 μm range, whereas the threshold size for particles to mainly travel in suspension is 70.00 μm (Haynes and Fanni, 2025). Thus, the fine sand (100.00–250.00 μm) represents the saltation load, and the finer fractions (less than 70.00 μm) represent the suspended matter. Our findings demonstrated that particles in the 100.00–250.00 μm range constitute the volumetrically dominant fraction both within nebkha deposits and on inter-shrub surfaces colonized by *T. mongolica* shrubs, confirming the effective interception of saltating particles. Situated within the grassland–desert ecotone—a critical desertification gradient—*T. mongolica* communities exhibit significant depletion of silt–clay fractions (less than 50.00 μm) and concurrent enrichment of fine sand (100.00–250.00 μm) in surface sediments (Jin et al., 2013). This pattern reflects the selective winnowing of fine suspendable particles, coupled with preferential trapping of saltation-sized particles, indicating that shrub branch architecture actively restructures particle size distribution by sieving the mobile grain population.

In desert transition zones, the ontogenetic development of *T. mongolica* enhances aerodynamic roughness through architectural augmentation, which includes the proliferation of surface branches while simultaneously increasing their angles and lengths. This process expands crown width and intensifies near-surface flow perturbation. Consequently, as crown dimensions increase, nebkha sediments exhibit a coarsening mean particle size alongside enriched fine-grained components (Lancaster and Baas, 2015). PCA results indicated that *T. mongolica* facilitates nebkha accumulation by intercepting particles within the 50.00–100.00 μm range, which can be attributed to increased branch ratios and elongated lower-layer branches. Paradoxically, the sediments of nebkha are depleted of very fine fraction (less than 50.00 μm) but enriched in coarser fractions (250.00–1000.00 μm) when compared to surrounding matrices. In the transitional zones between steppe and desert, the content of fine soil particles is higher due to the mixing of sand and grassland soil. The impact of bouncing particles can release sand from the surface, which can contribute to the production of further fine sediments. This difference arises from opposing aeolian fluxes: shrub branch architecture traps saltation-sized particles, but concurrent deflation of dust from the nebkha surface preferentially winnows fine suspendable particles. This mechanism has been observed in the oasis–desert nebkhas of Northwest China (Sweeney et al., 2016), explaining the particle size fining from nebkha interiors to peripheries (Zhang et al., 2020).

As a tertiary Mediterranean relict, *T. mongolica* embodies a protracted evolutionary history that manifests in complex above- and belowground feedback with aeolian geomorphology. This study demonstrated that shrub branch architecture modulates near-surface airflow to selectively trap saltation-sized particles, initiating and sustaining nebkha formation. However, the plant's extensive rooting system, which might have developed adventitious rootogenesis through chronic sand burial, is an unmeasured factor but can have a stabilizing effect. Constrained by short-term observation windows, this study did not address the contribution of shrub roots and adventitious roots to the formation and development of nebkhas. In future research, monitoring should be coupled with root system excavation and dating to help understand coupled ontogenetic processes above and below ground and their role in driving nebkha formation over the species' lifetime.

## 5 Conclusions

*T. mongolica* shrubs growing on the Ordos Plateau in China usually form stable nebkha around their crowns by trapping wind-blown sand. Based on this phenomenon, we conducted a comprehensive study on the changes in the significant branch architectures that constitute the canopy. The results indicated that with outward branch expansion, the branch ratios initially increased and then decreased. This decrease in branch length was accompanied by an increase in both branch angle and the ratio of branch diameters. Additionally, a significant positive

correlation was identified between crown area and nebkha size. The windward side of the shrub acted as a cross-section directly exposed to the direction of sand transportation, and its silhouette area showed a significant positive correlation with both nebkha bottom area and volume. Notably, the silhouette area of the 10–30 cm height layer most prominently influenced the nebkha deposition process. Path analysis revealed that the branch ratio, length, and angle, as well as the ratio of branch diameters near the ground surface were key branch architectures that affecting the crown area. Furthermore, this study confirmed that the sediments on both the interior and exterior surface of the crown are predominantly composed of fine sand, specifically within the range of 100.00–250.00 μm. Notably, the branch ratio, length, and angle near the ground surface redistributed sand particles within the 50.00–100.00 μm size range, thereby facilitating nebkha deposition. This study focused solely on the effect of shrub architecture on nebkha accumulation, excluding the roles of root systems and adventitious roots in nebkha formation and development. Future research should investigate the relationship between belowground root architecture and nebkha stabilization, as well as conduct long-term, multi-regional observations to clarify sediment sources and migration pathways in *T. mongolica* communities.



## Conflict of interest

The authors declare that they have no known competing financial interests or personal relationships that could have appeared to influence the work reported in this paper.

## Acknowledgements

This research was funded by the Natural Science Foundation of Inner Mongolia Autonomous Region (2024QN04023), the National Natural Science Foundation of China (41967009), the Research Program of Science and Technology at Universities of Inner Mongolia Autonomous Region "The Regulatory Mechanism of Near-Natural Vegetation Restoration on Sediment Carbon Sequestration Effects in Photovoltaic Power Stations in Desert Areas", and the Jining Normal University Doctoral Innovation Research Fund (jsbsjj2412). We thank Mr. ZHAO Naqi and Dr. GAO Junliang from the Experimental Center for Desert Forestry of Chinese Academy of Forestry for their support in the experimental process.

## Author contributions

Conceptualization: ZHAI Bo, DANG Xiaohong; Data curation: ZHAI Bo, DANG Xiaohong, LIU Xiangjie; Formal analysis: ZHAI Bo, LIU Jing, CHEN Xiaona; Funding acquisition: ZHAI Bo, DANG Xiaohong; Investigation: ZHAI Bo, DANG Xiaohong, LIU Jing, LIU Xiangjie, CHEN Xiaona, LIU Yajing; Methodology: ZHAI Bo, LIU Jing, LIU Xiangjie, CHEN Xiaona, LIU Yajing; Project administration: DANG Xiaohong; Resources: ZHAI Bo, DANG Xiaohong; Software: ZHAI Bo, LIU Jing, CHEN Xiaona, LIU Yajing; Supervision: DANG Xiaohong; Validation: ZHAI Bo, LIU Jing, LIU Xiangjie, CHEN Xiaona; Visualization: ZHAI Bo, LIU Xiangjie, LIU Yajing; Writing - original draft: ZHAI Bo; Writing - review and editing: ZHAI Bo, DANG Xiaohong, LIU Xiangjie, CHEN Xiaona. All authors approved the manuscript.

## References

Araus J L, Kefauver S C, Díaz O V, et al. 2022. Crop phenotyping in a context of global change: What to measure and how to do it. Journal of Integrative Plant Biology, 64(2): 592–618.

Awogbemi C A, Alagbe S A, Oloda F S. 2022. On the path analysis techniques and decomposition of correlation coefficients. Asian Journal of Probability and Statistics, 20(4): 208–219.

Barthélémy D, Caraglio Y. 2007. Plant architecture: a dynamic, multilevel and comprehensive approach to plant form, structure and ontogeny. Annals of Botany, 99(3): 375–407.

Bazzaz F A. 1979. The physiological ecology of plant succession. Annual Review of Ecology, Evolution, and Systematics, 10(1): 351–371.

Borchert R, Slade N. 1981. Bifurcation ratios and the adaptive geometry of trees. Botanical Gazette, 142(3): 394–401.

Chambers S M. 2020. Novel methodologies to disentangle plant–environment interactions. Applications in Plant Sciences, 8(2): e11324, doi: 10.1002/aps3.11324.

Chang Z F, Zhang J H, Shi X G, et al. 2017. Initial research on the relationship between sand-mound formation and the layered

silhouette of desert plants. Acta Ecologica Sinica, 37(21): 7351–7358. (in Chinese)

Cheng H, Zhang K D, Liu C C, et al. 2018. Wind tunnel study of airflow recovery on the lee side of single plants. Agricultural and Forest Meteorology, 263: 362–372.

Ciancio M E, Guida-Johnson B, Zuleta G A, et al. 2022. Rehabilitation planning in an oilfield in the Monte Austral: Mapping sand-sized sediment availability and assessing its effect on microtopography rehabilitation. Earth Surface Processes and Landforms, 47(13): 3133–3146.

Clark C B, Ma J X. 2023. The genetic basis of shoot architecture in soybean. Molecular Breeding, 43: 55, doi: 10.1007/s11032-023-01391-3.

Costas S, Sousa L B D, Gallego-Fernández J B, et al. 2024. Foredune initiation and early development through biophysical interactions. Science of The Total Environment, 940: 173548, doi: 10.1016/j.scitotenv.2024.173548.

Dos Santos P, Brilhante M A, Messerschmid T F E, et al. 2022. Plant growth forms dictate adaptations to the local climate. Frontiers in Plant Science, 13: 1023595, doi: 10.3389/fpls.2022.1023595.

El-Sheikh M A, Abbadi G A, Bianco P M, et al. 2010. Vegetation ecology of phytogenic hillocks (nabkhas) in coastal habitats of Jal Az-Zor National Park, Kuwait: Role of patches and edaphic factors. Flora, 205(12): 832–840.

Enquist B J, Brown J H, West G B. 1998. Allometric scaling of plant energetics and population density. Nature, 395: 163–165.

Fisher J B, Honda H. 1979. Branch geometry and effective leaf area: a study of *Terminalia*-branching pattern. 1. Theoretical trees. American Journal of Botany, 66(6): 633–644.

Goudie S. 2022. Nebkhas: An essay in aeolian biogeomorphology. Aeolian Research, 54: 100772, doi: 10.1016/j.aeolia.2022.100772.

Guan Q Y, Zhang J D, Wang L J, et al. 2013. Discussion of the relationship between dustfall grain size and the desert border, taking the southern border of the Tengger Desert and the southern dust deposit area as an example. Palaeogeography, Palaeoclimatology, Palaeoecology, 386(17): 1–7.

Haynes M, Fanni R. 2025. Development of a laboratory wind tunnel to test tailings erosion mechanisms. In: Knutsson S, Fourie A B, Tibbett M. Mine Closure 2025: Proceedings of the 18th International Conference on Mine Closure, Australian Centre for Geomechanics. Perth, Australia. doi: 10.36487/ACG_repo/2515_90.

He M Z, Wang H, Zhang J G, et al. 2005. Classification of the branching architectures of the desert plants in Minqin County. Acta Botanica Boreali-Occidentalia Sinica, 25(9): 1827–1832. (in Chinese)

Hesp P A. 1981. The formation of shadow dunes. Journal of Sedimentary Research, 51(1): 101–112.

Hildebrand M, Perles-Garcia M D, Kunz M, et al. 2021. Tree-tree interactions and crown complementarity: the role of functional diversity and branch traits for canopy packing. Basic and Applied Ecology, 50: 217–227.

Honda H. 1971. Description of the form of trees by the parameters of the tree-like body: Effects of the branching angle and the branch length on the shape of the tree-like body. Journal of Theoretical Biology, 31(2): 331–334.

Hu G Y, Dong Z B, Lu J F, et al. 2021. Spatial pattern of aeolian desertification and its causes in the Yellow River catchment. Journal of Desert Research, 41(4): 213–224. (in Chinese)

Jin Z, Dong Y S, Qi Y C, et al. 2013. Characterizing variations in soil particle-size distribution along a grass-desert shrub transition in the Ordos Plateau of Inner Mongolia, China. Land Degradation & Development, 24(2): 141–146.

Kidron G J, Zohar M. 2016. Factors controlling the formation of coppice dunes (nebkhas) in the Negev Desert. Earth Surface Processes and Landforms, 41(7): 918–927.

Koller A, Kunz M, Perles-Garcia M D et al. 2025. 3D structural complexity of forest stands is determined by the magnitude of inner and outer crown structural attributes of individual trees. Agricultural and Forest Meteorology, 363: 110424, doi: 10.1016/j.agrformet.2025.110424.

Lancaster N, Baas A. 2015. Influence of vegetation cover on sand transport by wind: Field studies at Owens Lake, California. Earth Surface Processes and Landforms, 23(1): 69–82.

Leopold L B. 1971. Trees and streams: the efficiency of branching patterns. Journal of Theoretical Biology, 31(2): 339–354.

Li J C, Yao Q, Wang Y, et al. 2019. Grain-size characteristics of surface sediments of nebkhas at the southern margin of the Mu Us dune field, China. CATENA, 183: 104210, doi: 10.1016/j.catena.2019.104210.

Li J R, Ravi S. 2018. Interactions among hydrological-aeolian processes and vegetation determine grain-size distribution of sediments in a semi-arid coppice dune (nebkha) system. Journal of Arid Environments, 154(7): 24–33.

Li S H, Mason J A, Xu Y H, et al. 2021. Biogeomorphology of nebkhas in the Mu Us dune field, north-central China: Chronological and morphological results. Geomorphology, 394: 107979, doi: 10.1016/j.geomorph.2021.107979.

Liu J W, Li Z Z, Wu S L, et al. 2009. The spatial heterogeneity of morphologic feature of *Nitraria* nebkhas around Ebinur Lake, Xinjiang. Journal of Desert Research, 29(4): 628–635. (in Chinese)

Liu Z K, Wang C W, Yang X J, et al. 2023. The relationship and influencing factors between endangered plant *Tetraena mongolica* and soil microorganisms in West Ordos desert ecosystem, northern China. Plants, 12(5): 1048, doi: 10.3390/plants12051048.

Lu Y, Zhang B R, Zhang M, et al. 2023. Relict plants are better able to adapt to climate change: Evidence from desert shrub communities. Plants, 12(23): 4065, doi: 10.3390/plants12234065.

Niklas K J, Cobb E D. 2010. Ontogenetic changes in the numbers of short- vs. long-shoots account for decreasing specific leaf area in *Acer rubrum* (Aceraceae) as trees increase in size. American Journal of Botany, 97(1): 27–37.

Osada N. 2006. Crown development in a pioneer tree, rhus trichocarpa, in relation to the structure and growth of individual branches. New Phytologist, 172(4): 667–678.

Pang Y J, Wu B, Jia X H, et al. 2022. Wind-proof and sand-fixing effects of *Artemisia ordosica* with different coverages in the Mu Us Sandy Land, northern China. Journal of Arid Land, 14(8): 877–893.

Qu Z Q, Liu L Y, Lü Y L. 2011. Psammophyte architecture and its relations with anti-wind erosion capability: a review. Chinese Journal of Ecology, 30(2): 357–362. (in Chinese)

Qu Z Q, Li Z G, Hu L X, et al. 2022. The branching architecture of *Artemisia ordosica* and its resistance to wind erosion. Frontiers in Environmental Science, 10: 960969, doi: 10.3389/fenvs.2022.960969.

Savinov I A. 2020. Architectural analysis of representatives of the Celastrales order: structure and rhythm of shoot development in connection with adaptations of species to different environmental conditions. Contemporary Problems of Ecology, 13: 300–308.

Steingraeber D A, Kascht L J, Franck D H. 1979. Variation of shoot morphology and bifurcation ratio in sugar maple (*Acer saccharum*) saplings. American Journal of Botany, 66(4): 441–445.

Steingraeber D A, Waller D M. 1986. Non-stationarity of tree branching patterns and bifurcation ratios. Proceedings of the Royal Society B: Biological Sciences, 228(1251): 187–194.

Sweeney M R, Lu H Y, Cui M C, et al. 2016. Sand dunes as potential sources of dust in northern China. Science China Earth Sciences, 59: 760–769.

Tengberg A. 1995. Nebkha dunes as indicators of wind erosion and land degradation in the Sahel zone of Burkina Faso. Journal of Arid Environments, 30(3): 265–282.

Valladares F, Gianoli E, Gómez J M. 2007. Ecological limits to plant phenotypic plasticity. New Phytologist, 176(4): 749–763.

White J. 1979. The plant as a metapopulation. Annual Review of Ecology, Evolution, and Systematics, 10(1): 109–145.

Whitney G G. 1976. The bifurcation ratio as an indicator of adaptive strategy in woody plant species. Bulletin of the Torrey Botanical Club, 103(2): 67–72.

Wolfe S A, Nickling W G. 1993. The protective role of sparse vegetation in wind erosion. Progress in Physical Geography, 17(1): 50–68.

Wu W Y, Zhang D S, Tian L H, et al. 2023. Morphological change and migration of revegetated dunes in the Ketu Sandy Land of the Qinghai Lake, China. Journal of Arid Land, 15(7): 827–841.

Xu D L, Yu X W, Chen J, et al. 2023. Arbuscular mycorrhizae fungi diversity in the root–rhizosphere–soil of *Tetraena mongolica*, *Sarcozygium xanthoxylon*, and *Nitraria tangutorum* Bobr in western Ordos, China. Agronomy, 13(6): 1485, doi: 10.3390/agronomy13061485.

Xu X J, Chen N M, Feng J C, et al. 2020. Comparative analyses of leaf cuticular lipids of two succulent xerophytes of the Ordos Plateau (Gobi Desert), *Tetraena mongolica* Maxim and *Zygophyllum xanthoxylum* (Bunge) Engl. Environmental and Experimental Botany, 177: 104129, doi: 10.1016/j.envexpbot.2020.104129.

Yagi T. 2006. Relationships between shoot size and branching patterns in 10 broad-leaved tall tree species in a Japanese cool-temperate forest. Canadian Journal of Botany, 84(12): 1894–1907.

Yan P, Deng Y H, An S J, et al. 2025. Training systems affect spatial distribution of Korla fragrant pear (*Pyrus sinkiangensis* Yu) fruits by altering canopy structure and light distribution. Frontiers in Plant Science, 16: 1615019, doi: 10.3389/fpls.2025.1615019.

Yang L W, Zhu S, Xu J. 2022. Roles of auxin in the inhibition of shoot branching in 'Dugan' fir. Tree Physiology, 42(7): 1411–1431.

Zhai B. 2022. The influence of the shrub configuration features of *Tetraena mongolica* Maxim on the aeolian processes and sedimentary characteristics. PhD Dissertation. Hohhot: Inner Mongolia Agricultural University. (in Chinese)

Zhang Z C, Han L Y, Pan K J, et al. 2020. Nebkha dune morphology in the gobi deserts of northern China and potential implications for dust emission. Sedimentology, 67(7): 3769–3782.

Zhao X H, Miao Z, Li F R, et al. 2025. Unraveling the individual and interactive effects of climate and competition on branch growth dynamics in *Pinus koraiensis* in Northeast China. Frontiers in Plant Science, 16: 1545892, doi: 10.3389/fpls.2025.1545892.

Zhu G N, Nong H J, Fang S Y, et al. 2024. Arbuscular mycorrhizal symbiosis reshapes the drought adaptation strategies of a dominant sand-fixation shrub species in northern China. Science of The Total Environment, 955: 177135, doi: 10.1016/j.scitotenv.2024.177135.

## Appendix

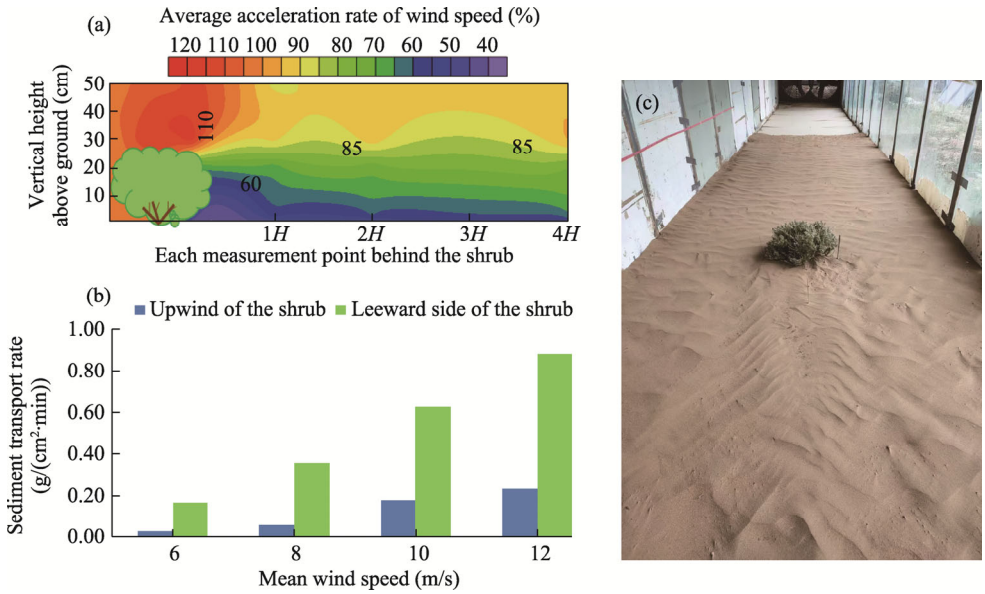


**Fig. S1** Wind tunnel simulation test to examine the effects of *T. mongolica* shrubs on wind speed, sand transport disturbance, and nebkha accumulation. (a), average acceleration rate of wind speed at different heights behind the shrub cluster when the incident wind speeds are 6.0, 8.0, 10.0, and 12.0 m/s; (b), sediment transport rate at heights ranging from 0 to 50 cm behind the shrub; (c), a small wind shadow sand pile formed beneath and behind the shrub after the wind tunnel simulation test. *H*, shrub height (*H*=27.00 cm in this study).